The University of
Nottingham

UNITED KINGDOM · CHINA · MALAYSIA

Roper, Ian P.E. and Besley, Nicholas A. (2016) The effect of basis set and exchange-correlation functional on time-dependent density functional theory calculations within the Tamm-Dancoff approximation of the X-ray emission spectroscopy of transition metal complexes. Journal of Chemical Physics . ISSN 1089-7690 (In Press)

Access from the University of Nottingham repository:
http://eprints.nottingham.ac.uk/32079/1/jcp-xes-final.pdf

For more information, please contact

The Effect of Basis Set and Exchange-Correlation Functional on Time-Dependent Density Functional Theory Calculations within the Tamm-Dancoff Approximation of the X-Ray Emission Spectroscopy of Transition Metal Complexes

Ian P. E. Roper[1] and Nicholas A. Besley[1, a)]

School of Chemistry, University of Nottingham, University Park, Nottingham,

NG7 2RD, UK.

The simulation of X-ray emission spectra of transition metal complexes with time-dependent density functional theory (TDDFT) is investigated. X-ray emission spectra can be computed within TDDFT in conjunction with the Tamm-Dancoff approximation by using a reference determinant with a vacancy in the relevant core orbital, and these calculations can be performed using the frozen orbital approximation or with the relaxation of the orbitals of the intermediate core-ionised state included. Both standard exchange-correlation functionals and functionals specifically designed for X-ray emission spectroscopy are studied, and it is shown that the computed spectral band profiles are sensitive to the exchange-correlation functional used. The computed intensities of the spectral bands can be rationalised by considering the metal p orbital character of the valence molecular orbitals. To compute X-ray emission spectra with the correct energy scale allowing a direct comparison with experiment requires the relaxation of the core-ionised state to be included and the use of specifically designed functionals with increased amounts of Hartree-Fock exchange in conjunction with high quality basis sets. A range-corrected functional with increased Hartree-Fock exchange in the short range provides transition energies close to experiment and spectral band profiles that have a similar accuracy to those from standard functionals.

a)nick.besley@nottingham.ac.uk

I. INTRODUCTION

X-ray emission spectroscopy (XES) arises from the decay of valence electrons to fill vacant core orbitals following ionisation of core electrons. XES probes the occupied molecular orbitals and is complementary to X-ray absorption spectroscopy (XAS) which is sensitive to the unoccupied orbitals. Owing to the nature of core orbitals, these techniques provide an element specific, local probe of geometric and electronic structure. XES is becoming an increasingly important technique due to improved X-ray sources and the development of X-ray free-electron lasers that can deliver short femtosecond pulses of hard X-rays which hold the promise of resolving ultrafast chemical processes at an atomic level.[1,2]

Recent work has demonstrated the value of XES for the study of transition metal complexes, and experimental spectra for Fe, Cr, Ti and Mn based complexes have been reported.[3–11] XES is sensitive to the nature of the bonding in transition metal complexes, giving information on the coordination environment and the potential to identify coordinated ligands. For example, XES measurements showed there to be a central carbon in the nitrogenase iron-molybdenum cofactor.[12] For transition metal complexes, XES is usually studied following the ionisation of a metal 1s electron. The most prominent features in the corresponding spectra are the $K\beta_{1,3}$ emission lines which are associated with electric dipole allowed metal 3p→1s transitions. Much of the experimental work has focused on higher energy transitions that have significantly lower intensity. This region is referred to as the valence to core region and comprises transitions from orbitals associated with the ligands. There are two groups of features in this region, the $K\beta''$ lines that arise from ligand-valence s→metal 1s transitions and the $K\beta_{2,5}$ lines corresponding to ligand-valence p→metal 1s transitions.[4]

Calculations of XES have an important role in interpreting experimental spectra and assigning the observed bands. Several approaches to computing XES have been adopted, in ligand field multiplet theory a single ion is considered and the chemical environment is then incorporated empirically by introducing the crystal field splittings and the orbital mixing.[13] The energy and matrix elements of the electric dipole moment operator for the various valence to core transitions required to simulate an X-ray emission spectrum can be evaluated

2

using a variety of methods including semi-empirical, Hartree-Fock (HF),[14] configuration interaction (CI),[15] multi-configurational self-consistent field (MCSCF) wave functions,[16,17] Monte Carlo configuration interaction,[18] as well as Kohn-Sham density functional theory (DFT).[4] Following ionisation of a core electron there is some relaxation of the electronic structure, and various approaches to describing the orbitals of the core-excited state have been adopted. These range from a frozen orbital (FO) approximation where the ground state orbitals are used,[4,19–21] Z+1 approximation where an increased nuclear charge is used for the absorbing atom,[3] the transition potential approach where a half filled core orbital is used providing a balance between final and initial states[19,22,23] and a fully relaxed approach where the orbitals of the core-hole state are optimised in separate self-consistent field (SCF) calculations.[24,25] This latter approach has the limitations that individual SCF calculations are necessary for all of the relevant states and the resulting wave functions are not orthogonal. X-ray emission spectroscopy has been computed using a real-space-grid projector augmented wave framework which can be used to study large systems[26] and recent work has shown how to include vibrational interference effects in the simulation of the spectra.[27]

Within the context of transition metal complexes, the simulation of spectra has been predominantly based upon DFT calculations. Smolentsev et al.[3] computed X-ray emission spectra of Mn complexes with DFT and the core-hole described using the Z+1 approximation. The generalised gradient approximation Perdew-Wang exchange-correlation functional was used and the predicted spectra was shifted to align with experiment. The calculations allowed features in the valence to core region could be assigned to orbitals mainly localised on the ligands. More recent DFT calculations on Fe complexes used the FO approximation with the transition energies given by the difference in the corresponding orbital energies and the intensities evaluated from the matrix elements of the electric dipole, electric quadrupole and magnetic dipole operators.[4] These calculations demonstrated good agreement with the experimental data, reproducing the shape of the spectral bands in the valence to core region. Similar protocols have been applied to study manganese complexes,[6,10] chromium complexes[11] and substituted ferrocenes.[8]

Recently it was shown that X-ray emission spectra can be computed with equation of motion coupled cluster with single and double excitations (EOM-CCSD) and time-dependent

density functional theory (TDDFT) methods by using a reference determinant for the ionised state that has a core-hole.[28–30] With this reference determinant the transitions to the vacant core orbital appear as negative eigenvalues. EOM-CCSD provides accurate transition energies (within about 0.5 eV) for transitions at the K-edge of first and second row elements. However, converging the CCSD equations with a core-hole reference wave function can be problematic and the computational cost of this method makes it unsuitable for application to transition metal complexes.[30,31] Provided that the Tamm-Dancoff approximation (TDA) is imposed,[32] TDDFT can be applied to a reference determinant with a core-hole. TDDFT has the advantage that all of the necessary states are computed in the same calculation making it easy to use and also avoiding issues with the non-orthogonalilty of the states, and TDDFT calculations of XES can be performed within the FO or Z+1 approximations. TDDFT has a significantly lower computational cost and can be readily applied to study the XES of large transition metal complexes. Recently Zhang *et al.* extended TDDFT calculations of XES to consider transition metal complexes.[33] These calculations studied a range of chromium, manganese and iron based complexes with the B3LYP exchange-correlation functional in conjunction with the Sapporo-TZP-2012[34] basis set for the metal and 6-311G** basis set for the ligands with the spectral bands shifted to align with experiment. Overall, the computed spectral profiles provided a reliable description of the experimental data.

In this paper we explore the application of TDDFT/TDA to compute X-ray emission spectra of transition metal complexes, focusing on the dependence of the computed spectra to the frozen orbital approximation, choice of exchange-correlation functional and basis set in an effort to compute spectra with the correct energy scale. This can provide greater confidence in the assignment of bands in complex spectra and also be important when comparing small shifts in peak positions between different systems where the magnitude of the shift can be of the order of the error in the constant shift applied. To achieve this requires the relaxation of the molecular orbitals in the presence of the core-hole to be included, high quality basis sets, relativistic effects and also specifically designed exchange-correlation functionals to be considered. Standard exchange-correlation functionals give excitation energies that are significantly too large compared with experimental data.[28,30] This is complementary to TDDFT calculations of XAS, where the predicted excitations energies are too low.[35,36] There has been significant progress in the design of exchange-correlation functionals for the

4

calculations of XAS based upon tailoring the fraction of exact Hartree-Fock (HF) exchange in the functional.[35–38] In particular, the introduction of HF exchange in the short range is important.[38] We also develop a quantitative relationship between the nature of the occupied orbitals and the intensity of the spectral bands.

II. COMPUTATIONAL METHODS

Within TDDFT X-ray emission transitions energies and oscillator strengths can be computed with the following process:[30]

1. Perform an unrestricted Kohn-Sham DFT calculation for the ground state of the system (with appropriate charge and spin state).

2. Use the resulting molecular orbitals as the starting point for a further Kohn-Sham DFT calculation with a core hole in the relevant orbital, using an overlap criterion[39,40] to prevent the collapse of the core hole during the SCF process. The FO approximation can be invoked by by-passing this second SCF calculation.

3. Perform a standard TDDFT/TDA calculation and the X-ray emission transitions appear as negative eigenvalues with the associated oscillator strengths.

In TDDFT with the TDA[32] the transition energies correspond to solutions of the following eigenvalue equation

$$\mathbf{A}\mathbf{X} = \omega\mathbf{X} \tag{1}$$

The matrix $\mathbf{A}$ is given by

$$A_{ia\sigma,jb\tau} = \delta_{ij}\delta_{ab}\delta_{\sigma\tau}(\epsilon_{a\sigma} - \epsilon_{i\tau}) + (ia\sigma|jb\tau) + (ia\sigma|f_{XC}|jb\tau) \tag{2}$$

where

$$(ia\sigma|jb\tau) = \int\int \psi_{i\sigma}^*(\mathbf{r}_1)\psi_{a\sigma}^*(\mathbf{r}_1)\frac{1}{r_{12}}\psi_{j\tau}(\mathbf{r}_2)\psi_{b\tau}(\mathbf{r}_2)d\mathbf{r}_1 d\mathbf{r}_2 \tag{3}$$

$$(ia\sigma|f_{XC}|jb\tau) = \int \psi_{i\sigma}^*(\mathbf{r}_1)\psi_{a\sigma}(\mathbf{r}_1)\frac{\partial^2 E_{XC}}{\partial\rho_\sigma(\mathbf{r}_1)\partial\rho_\tau(\mathbf{r}_2)}\psi_{j\tau}(\mathbf{r}_2)\psi_{b\tau}^*(\mathbf{r}_2)d\mathbf{r}_1 d\mathbf{r}_2 \tag{4}$$

5

and ϵ_i are the orbital energies and E_{XC} is the exchange correlation functional. We note that use of the TDA is necessary for these calculations since full TDDFT calculations are not possible for the reference determinant with a core-hole and all of the TDDFT calculations presented have used the TDA. The TDA approximation only has a small effect on the computed transition energies but can have a more significant effect on the computed intensities. As the nuclear charge of the absorbing atom increases, scalar relativistic effects become increasingly important in calculations of X-ray spectroscopies at the K-edge. Relativistic effects result in a lowering of the energy of the 1s core orbital, and for transition metals this effect cannot be neglected. These effects are incorporated into the calculations by modifying the diagonal elements of $\mathbf{A}$ as follows

$$A_{ia\sigma,jb\tau} = \delta_{ij}\delta_{ab}\delta_{\sigma\tau}(\epsilon_{a\sigma} - \epsilon_{i\tau} - \Delta_R) + (ia\sigma|jb\tau) + (ia\sigma|f_{XC}|jb\tau) \qquad (5)$$

where Δ_R is the magnitude of the energy change in the core orbital energy due to relativistic effects. This has been computed as the difference in the 1s orbital energy between relativistic and non-relativistic HF/cc-pCVTZ for the relevant atom with the relativistic effects modelled using the Douglas-Kroll-Hess Hamiltonian, and a similar approach has been used to correct X-ray absorption transition energies.[41] The values of Δ_R show an increase with increasing nuclear charge with values of 38.41 and 44.68 eV for chromium and manganese, respectively. In this approach the lowering in energy owing to relativistic effects for the valence orbitals is neglected. These effects are much smaller than for the core orbitals and lie between 0.1 eV and 0.2 eV.

The B3LYP,[42,43] BP86[44,45] and modified hybrid and short-range corrected (SRC) functionals have been used to compute transition energies and spectra. For the K-edge of first and second row elements the following hybrid functional was shown to the accurate for XES where the fraction of HF exchange was optimised to reproduce accurate transition energies[30]

$$\text{B}^{66}\text{LYP} = 0.66 \text{ HF} + 0.26 \text{ B} + 0.08 \text{ S} + 0.19 \text{ VWN} + 0.81 \text{ LYP} \qquad (6)$$

where HF, B and S are Hartree-Fock, Becke and Slater exchange functionals, and VWN and LYP are correlation functionals.[44,46–48] A SRC functional has also been optimised for X-ray emission transitions. In a SRC functional there is a high fraction of the HF exchange

in the short range (low r_{12}) which falls of quickly as r_{12} increases. This functional has the following four parameters C_{SHF}=0.71, C_{LHF}=0.17, μ_{SR}=0.64 a$_{\text{o}}^{-1}$ and μ_{LR}=2.45 a$_{\text{o}}^{-1}$ which represent the fractions of HF exchange at r_{12}=0 and $r_{12}=\infty$, while μ_{SR} and μ_{LR} are the attenuation parameters in the error functions.

In addition to the exchange-correlation functional, another factor that has emerged as important is the nature of the basis functions present in the basis set. For ionisation of core electrons of heavier atoms, it is increasingly important to include additional basis functions for the core orbitals.[30] A range of basis sets have been studied including 6-31G*, 6-31G* with uncontracted core basis functions (denoted u6-31G*), Ahlrichs VTZ, cc-pVDZ, cc-pVTZ and cc-pCVTZ.[49-53] For the calculations denoted cc-pCVTZ, the cc-pwCVTZ basis set was used for the metal atom with the cc-pVTZ basis set used for the remaining atoms. All calculations were performed with the Q-Chem software package[54] and the structures were optimised at the B3LYP/6-31G* level. Spectra have been generated by convoluting the computed transitions with gaussian functions with bandwidth of 1.5 eV. Calculations are presented for the $[\text{MnO}_4]^{1-}$, $[\text{MnN(CN)}_4]^{2-}$, Cr(CO)_6 and $[\text{Cr(NH}_3)_6]^{3+}$ complexes since they are relatively small to allow calculations with large basis sets and have high quality experimental data available. Comparison of the calculated results with experiment for these clusters allows the general trends in the accuracy of the calculations with respect to the exchange-correlation functional and basis set to be established. In the calculations presented, the effects of spin multiplet states are not included. Multiplet effects in X-ray spectroscopy have been reviewed and found to be less important for K-edge transitions compared to L-edge transitions.[55]

For the analysis of the results it is useful to quantify the metal p orbital character of the molecular orbitals. The metal p orbital character in an orbital i is evaluated as

$$P_i = \sum_{\bar{\mu}} \left(c_{\bar{\mu}i} \right)^2 \tag{7}$$

where $\bar{\mu}$ runs over the p orbital basis functions of the central metal atom and $c_{\bar{\mu}i}$ are the molecular orbital coefficients. The metal p orbital character in a transition to give final state λ is defined as

$$T_p^\lambda = \sum_i \left(\kappa_{ic} \right)^2 P_i \tag{8}$$

7

where κ_{ic} is the TDDFT amplitude for the transition from molecular orbital i to the metal core orbital for the state λ. In practice we include amplitudes with a magnitude greater than 0.1. The p character of a band in the spectrum (T_p) is determined from summing the T_p^λ for the electronic transitions that contribute to the band. We note that this type of analysis will become unreliable for basis sets which have extended (diffuse) p basis functions. In these cases the summation can be limited to include only the compact basis functions in the basis set, however, we have not explored this in detail in this work and all values of P_i are computed with the 6-31G* basis set.

III. RESULTS AND DISCUSSION

Initially we consider the sensitivity of the computed transition energies to the basis set and exchange-correlation functional. Table I shows the computed transition energies for the K$\beta_{1,3}$ line and the most intense transition in the K$\beta_{2,5}$ region for $[\text{MnO}_4]^{1-}$ with three different exchange-correlation functionals and basis sets of varying quality. We consider first the values for the B3LYP functional. For both transitions, the sensitivity of the computed transition energies to the size of the basis set is evident. There is a lowering of about 40 eV in the computed transition energy between the smallest (6-31G*) and the largest (cc-pCVTZ) basis sets used. However, with the cc-pCVTZ basis set the predicted transition energies remain over 50 eV too high, and this remaining error can be largely associated with the exchange-correlation functional. Table I also shows computed transition energies for the B^{66}LYP and SRC fun.ctionals that were parameterised based upon X-ray emission transitions following the photoionisation of the 1s electrons of first and second row elements. Both functionals demonstrate a similar dependence on the quality of the basis set. As expected, the functionals predict transition energies closer to the experimental values. With B^{66}LYP the predicted transition energy for the valence to core region with the larger basis set is 6544 eV compared to the experimental value of 6538 eV. The SRC functional gives the closest agreement with the experimental value with a predicted transition energy of 6537 eV for the K$\beta_{2,5}$ line.

Since the nuclear charge of first row transition metals is greater it follows that a higher

Method	K$\beta_{1,3}$	K$\beta_{2,5}$	$\Delta E_{K\beta_{2,5}}$
B3LYP/6-31G*	6587	6636	+98
B3LYP/u6-31G*	6581	6629	+91
B3LYP/cc-pVDZ	6584	6633	+95
B3LYP/Ahlrichs VTZ	6551	6600	+62
B3LYP/cc-pVTZ	6569	6620	+82
B3LYP/cc-pCVTZ	6549	6597	+59
B^{66}LYP/6-31G*	6540	6582	+44
B^{66}LYP/u6-31G*	6533	6573	+35
B^{66}LYP/cc-pVDZ	6539	6580	+42
B^{66}LYP/Ahlrichs VTZ	6505	6545	+7
B^{66}LYP/cc-pVTZ	6525	6566	+28
B^{66}LYP/cc-pCVTZ	6503	6544	+6
SRC/6-31G*	6535	6576	+38
SRC/u6-31G*	6529	6571	+33
SRC/cc-pVDZ	6532	6572	+34
SRC/Ahlrichs VTZ	6499	6539	+1
SRC/cc-pVTZ	6515	6566	+28
SRC/cc-pCVTZ	6498	6537	-1
Exp.[a]	-	6538	-

TABLE I. Variation in the computed emission energies with functional and basis set for $[MnO_4]^{1-}$. $\Delta E_{K\beta_{2,5}}$ is the deviation of the calculated emission energy from experiment for the K$\beta_{2,5}$ line. [a]experimental data[10]. The number of basis functions for manganese are 36, 41, 43, 43, 68 and 127 for the 6-31G*, u6-31G*, cc-pVDZ, Ahlrichs VTZ, cc-pVTZ and cc-pCVTZ basis sets, respectively, and 15, 15, 14, 14, 30, 30 for oxygen.

fraction of HF exchange than 66% in a hybrid functional may be optimal. However, we do not consider in detail increasing the fraction of HF exchange because, as is shown later, increasing the component of HF exchange can have a detrimental effect on the predicted band shapes. For the SRC functional the predicted transition energy is slightly lower than

experiment suggesting that increasing the HF component would worsen the agreement with experiment. This is similar to the case of XAS where exchange-correlation functionals parameterised for second row elements perform reasonably well for the K-edge of first row transition metals.[56,57] The cc-pCVTZ basis set represents a quite extensive basis set that cannot be readily applied to large transition metal complexes. The fact that a very large basis sets is required to converge the transition energies is largely due to the basis sets not being designed for core orbital properties. With appropriately designed basis sets it should be possible to converge the energy with a much smaller number of basis functions. An example of this are the IGLO basis sets[58] which are designed for NMR calculations, these work very well for the XES of first and second row elements but do not exist for transition metal elements. Amongst the smaller basis sets studied, we note that the Ahlrichs VTZ basis set also predict transition energies that are reasonably close to experiment.

We now consider how the different approximations and various exchange-correlation functionals affect the computed band profiles. Predicting the band profile is key to simulation of XES spectra. Since computed spectra can be shifted to align with experiment it is important that exchange-correlation functionals designed to predict the transition energies correctly do not do so at the expense of the computed band profile. Figure 1 shows the valence to core region computed with various exchange-correlation functionals and the large cc-pCVTZ basis set with the spectra shifted to align with the experimental data for the $[MnO_4]^{1-}$ complex. Also shown are the valence molecular orbitals that contribute to this region of the spectrum with their values for P_i evaluated using B3LYP/6-31G* (see equation 7). The P_i values do not vary significantly between different exchange-correlation functionals, for example the values for the two orbitals with the SRC functional are 0.045 and 0.032 compared to 0.049 and 0.034. The P_i values suggest that there are two orbitals that have a significant (> 0.01) metal orbital character and it is indeed transitions from these two orbitals that gives the two prominent bands observed in the spectrum.

The spectrum computed with B3LYP with the FO approximation, wherein the molecular orbitals are not relaxed within the second SCF calculation, has an accurate band profile and a relative energy spacing of the bands in good agreement with experiment. This is similar to a previously published spectrum which is computed based upon the Kohn-Sham orbitals
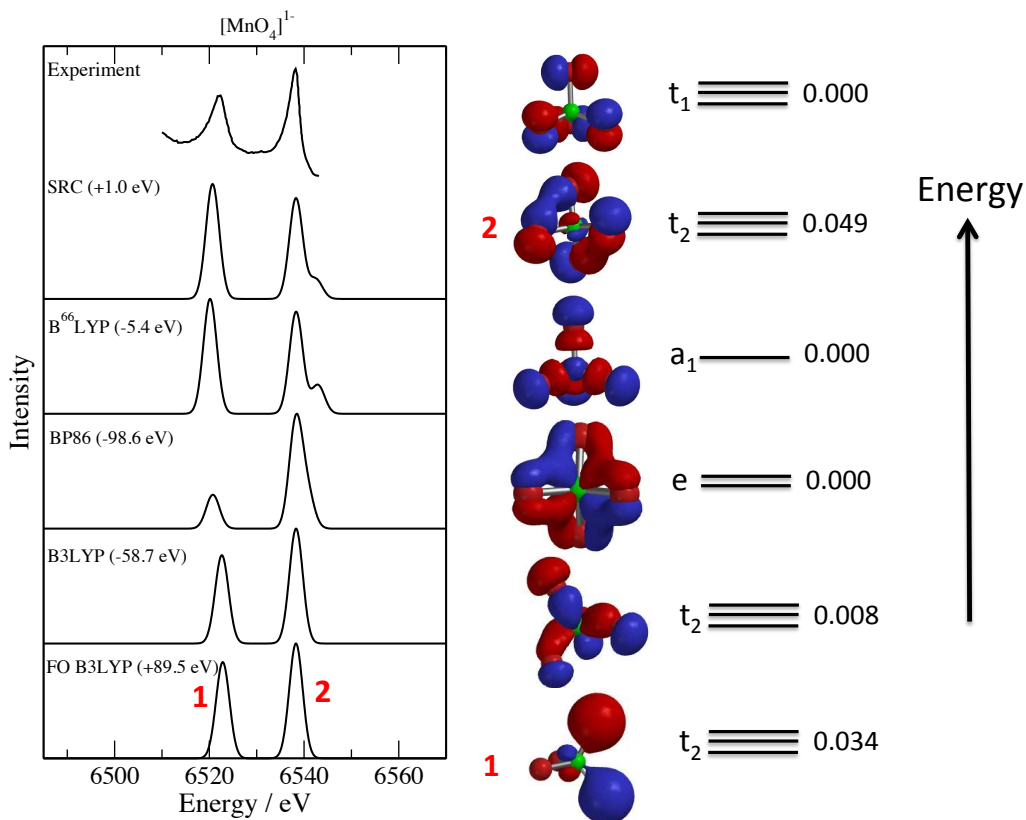
FIG. 1. Experimental and computed X-ray emission spectra for $[MnO_4]^{1-}$ with various exchange-correlation functionals and the cc-pCVTZ basis set shown with the valence molecular orbitals and their associated P_i values. The computed spectra have been shifted to align with experiment with the shifts applied shown in parenthesis. Experimental data adapted from reference[10].

of the ground state, and reflects the general success of these approaches to simulating XES spectra.[4,6,8,10,11] Removing the FO approximation has no noticeable effect on the shape of the spectral profile but it does result in a large shift in the transition energies. Removing a core electron increases the effective nuclear charge, which leads to a lowering in the energies of the molecular orbitals. This effect is greatest for the core orbitals resulting in an overall increase in the transition energies. Optimising the molecular orbitals in the presence of the core-hole also results in a lower oscillator strengths which correlates with a reduction in the metal p orbital character in the orbitals. This effect is greatest for the t_2 orbitals contributing to the lower energy band which is consistent with the small reduction in the intensity of this band relative to the more intense band when the FO approximation is

11

Molecule	Band Energy / eV	T_p SRC	$f \times 100$ SRC	T_p B3LYP	$f \times 100$ B3LYP
$[MnO_4]^{1-}$	6543	0.048	0.033	0.012	0.000
	6539	0.129	0.167	0.117	0.113
	6521	0.093	0.190	0.075	0.087

TABLE II. Calculated p orbital character in the observed bands and oscillator strengths for B3LYP and SRC exchange-correlation functionals.

removed. Using a different exchange-correlation functional BP86 results in a change in the relative intensity of the two bands, with the relative intensity of the higher energy band increasing.

The spectrum for B[66]LYP is much closer to the experiment in terms of the absolute transition energies, but a distinct peak emerges on the high energy side of the band at 6538 eV. The closest to experiment in terms of absolute energies is the SRC functional, and for this functional the resulting spectrum is in reasonable agreement with experiment. However, for this functional there is also a small shoulder at the base of the band at high energy. Closer inspection shows that this feature is also evident in an asymmetry in the band from the calculation with BP86. The corresponding transitions are present in the B3LYP calculation, but the band is not evident because the transitions have zero intensity. This contradicts the analysis in terms of the metal p character of the molecular orbitals and suggests that a band of significant intensity arises from a transition from an orbital with d orbital character at the central metal atom. This can be rationalised by considering the values of T_p for the spectral bands which are shown in Table II. This shows that there is a significant value of T_p for the band at 6543 eV for the SRC functional which is not given with the B3LYP functional. This demonstrates that this intensity arises from a mixing of transitions from orbitals with metal p character into this transition within the TDDFT calculation. The precise balance of ligand and metal character of the molecular orbitals and the TDDFT amplitudes (κ_{ic}) will be dependent on the exchange-correlation functional used and can rationalise the observed sensitivity of the band profiles to the functionals.

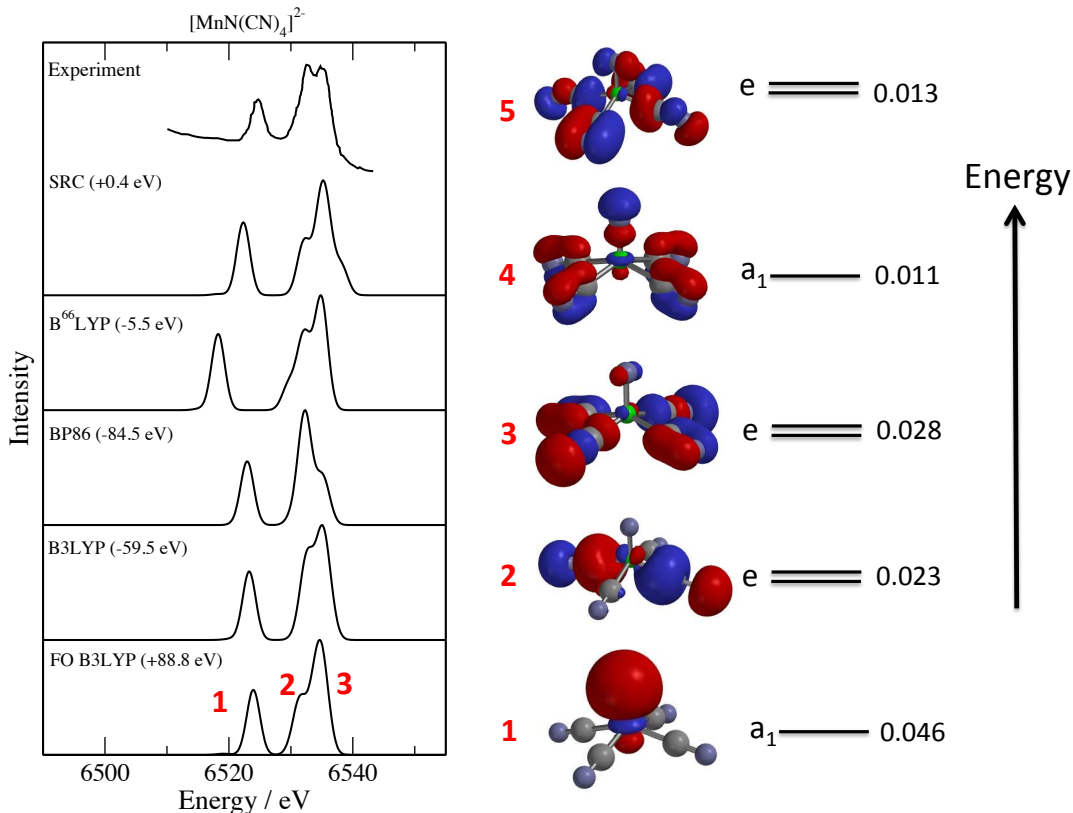Figure 2 shows a range of computed spectra for the $[MnN(CN)_4]^{2-}$ complex. The experi-

FIG. 2. Experimental and computed X-ray emission spectra for $[\mathrm{MnN(CN)_4}]^{2-}$ with various exchange-correlation functionals and the cc-pCVTZ basis set shown with the valence molecular orbitals with P_i values > 0.01. The computed spectra have been shifted to align with experiment with the shifts applied shown in parenthesis. Experimental data adapted from reference[10].

mental spectrum for this complex shows two distinct bands, the higher energy band is more intense with two peaks of similar intensity. For this complex there are five orbitals with significant metal p character that contribute to this region of the spectrum which are also shown in Figure 2. The peak at low energy is arises from an orbital of a_1 symmetry that is localised on the metal-nitrogen atom bond. The broader higher energy band has contributions from the other four orbitals, but with dominant contributions from two of these. The accurate description of this band represents a challenge since it requires the balance between these different contributions to be described correctly. The spectrum given by B3LYP with the FO approximation correctly predicts the energy separation between the two bands but the intensity of the lower energy component of the band at higher energy is too weak.
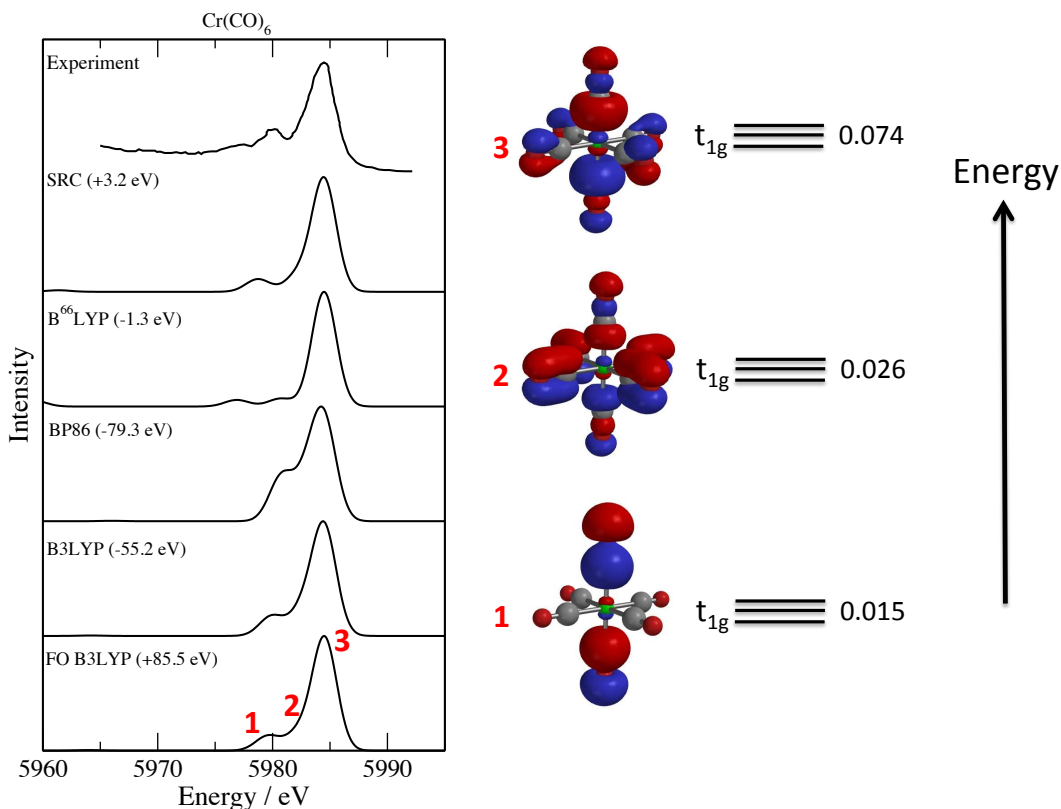
FIG. 3. Experimental and computed X-ray emission spectra for $Cr(CO)_6$ with various exchange-correlation functionals and the cc-pCVTZ basis set shown with the valence molecular orbitals with P_i values > 0.01. The computed spectra have been shifted to align with experiment with the shifts applied shown in parenthesis. Experimental data adapted from reference[11]

.

Removing the FO approximation gives a spectrum for B3LYP where the relative intensities of these two components is closer to the experimental data. For the remaining spectra computed with different exchange-correlation functionals there is significant variation in the relative intensities of these two peaks with the calculations showing one component to be more intense. Most of the calculations predict the separation between the two bands well with the exception of B66LYP functional which overestimates the separation. Overall for the Mn based complexes the best agreement with experimental data is given by the B3LYP functional without the FO approximation. The choice of exchange-correlation functional has a significant effect on the predicted band profiles. The functionals designed for XES
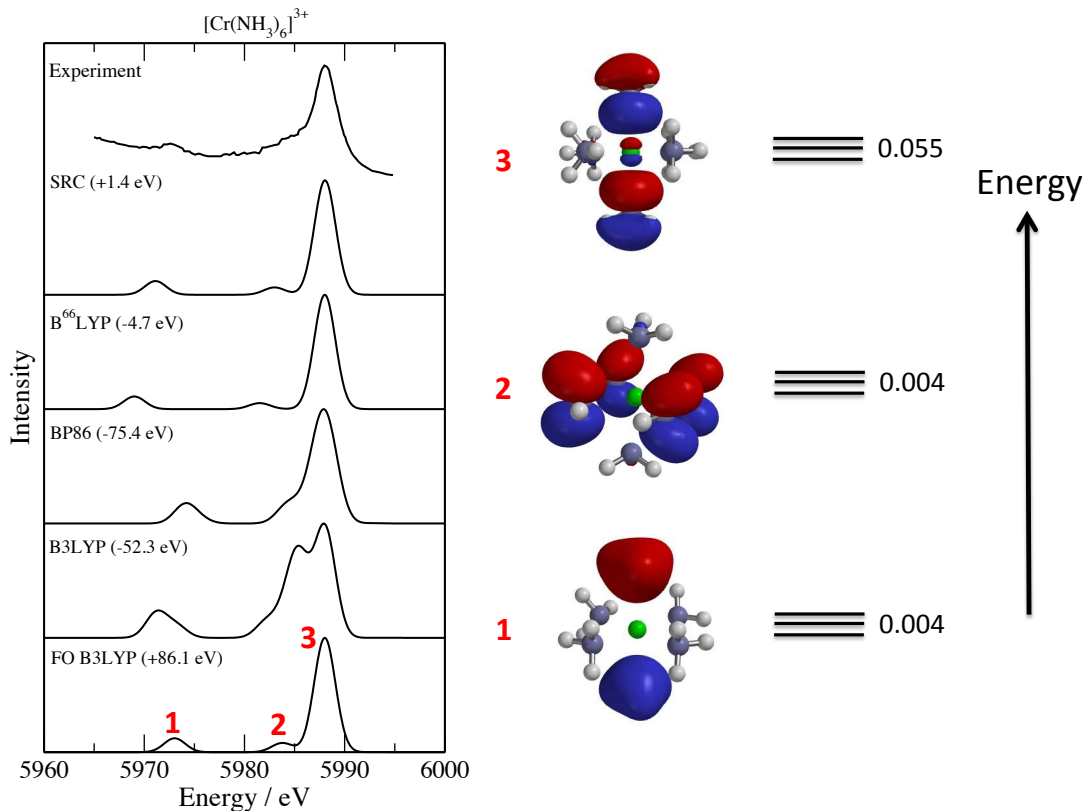
14

FIG. 4. Experimental and computed X-ray emission spectra for $[Cr(NH_3)_6]^{3+}$ with various exchange-correlation functionals and the cc-pCVTZ basis set shown with the relevant valence molecular orbitals. The computed spectra have been shifted to align with experiment with the shifts applied shown in parenthesis. Experimental data adapted from reference[11].

provide more accurate absolute energies but there is some worsening of the predicted band profiles, particularly for B^{66}LYP. This is likely due to the higher fraction of HF exchange worsening the description of the valence orbitals. The SRC functional by its nature provides a compromise since it corrects the transition energies with a smaller change in the band profile compared with B3LYP.

Figures 3 and 4 show computed spectra for two chromium based complexes $Cr(CO)_6$ and $[Cr(NH_3)_6]^{3+}$. The experimental spectrum of $Cr(CO)_6$ shows an intense band at 5985 eV with a shoulder on the low energy side with a weaker band about 5 eV lower in energy. The P_i analysis gives three t_{1g} orbitals with significant metal p orbital character with orbital with the orbital with highest energy having a significantly larger value. These three orbitals give

Molecule	Band Energy / eV	P_i	T_p	f	Experiment
$[\mathrm{MnO_4}]^{1-}$	6537	1.00	1.00	1.00	Most intense band
	6520	0.71	0.72	1.19	$\approx \frac{2}{3}$ as intense
$[\mathrm{Cr(NH_3)_6}]^{3+}$	5987	1.00	1.00	1.00	Most intense band
	5982	0.06	0.06	0.06	shoulder on the main band
	5973	0.05	0.05	0.12	$< \frac{1}{20}$ as intense

TABLE III. Relative intensities of the spectral bands computed with the SRC exchange-correlation functional.

the three features in the computed spectra with the orbital with $P_i = 0.074$ associated with the most intense band. Most of the calculations provide a good description of this spectrum. The exceptions to this are the BP86 functional, where the low energy feature appears as a large shoulder on the main band band, and the B^{66}LYP functional where the lower energy feature is too weak. In particular the spectrum computed with the SRC functional is close to experiment.

The three complexes studied so far have a singlet ground state with doublet core-excited state. $[\mathrm{Cr(NH_3)_6}]^{3+}$ is different in that it has a quartet ground state. For this system the core-hole is introduced with α spin where there is a greater number of α electrons. Analogous calculations with a core-hole of β spin can be performed, however, the resulting transitions have lower energies and do not contribute to the spectrum presented. One further issue with these calculations is that an unrestricted Kohn-Sham determinant for open-shell systems will suffer from spin-contamination. Spin-contamination is also an issue for ΔSCF calculations that allow for the relaxation of the orbitals in the presence of the core-hole. This is particularly the case for $[\mathrm{Cr(NH_3)_6}]^{3+}$ which has a triplet core-hole state. The results show that the SRC functional also describes the spectrum for the $[\mathrm{Cr(NH_3)_6}]^{3+}$ well. This suggests that the effects of spin-contamination in the reference wavefunction are not apparent in the resulting spectrum once that the line broadening has been applied or that the associated error is less significant than other approximations made in the calculations. However, it is clearly desirable to remove the spin-contamination from the calculations. A previous study that compared XES spectra computed using DFT with the B3LYP and BP86 functionals

found there to be only small differences between the intensities of the bands, although in the B3LYP spectra the bands were spread out more with a greater separation between the high and low energy features.[8] This is also evident in the TDDFT spectra shown here, although a greater variation in the intensities is observed here. It is possible that intensities computed with TDDFT are more sensitive to the exchange-correlation functional than spectra computed based upon single electron transitions and the Kohn-Sham orbitals. Within a TDDFT approach the transitions are no longer described as pure one electron transitions, and the mixing between one electron transitions can affect the computed intensity. The different functionals provide fairly consistent predictions of the spectrum for this complex, with some variation in the energy separation between the bands. For this complex B3LYP without the FO approximation shows the greatest deviation from experiment with the weak feature on the low energy side of the intense band predicted to be too intense. The ratio of the intensities of the bands in the spectra for $[MnO_4]^{1-}$ and $[Cr(NH_3)_6]^{3+}$ as predicted by the different approaches are given in Table III. These show that the values given by P_i and T_p are in close agreement with experiment and surprisingly closer to experiment than the TDDFT oscillator strength. This may in part be associated with the use of the TDA which is likely to lead to greater errors in the computed oscillator strengths or the dipole approximation which may also play a role.[59,60]

The aim of the B[66]LYP and SRC functionals is to predict the absolute energies of the transitions. Table IV summarises the computed positions of the prominent bands in the spectra for these two functionals. We will focus on the results for the SRC functional since this functional gives an overall better description of the spectral profiles. For the two manganese based complexes, the computed transition energies are close to the experimental values and a shift of 1 eV or less is required to align the computed and experimental spectra. There is a small increase in the error in the computed transition energies for the chromium based complexes. However considering other sources of error that are present in the calculations, for example the treatment of relativistic effects and the remaining incompleteness of the basis set, a reasonable level of accuracy is achieved. As discussed previously, the computed transition energies are strongly dependent on the basis set and to approach convergence with respect to the basis set requires large basis sets with tight basis functions suitable for described the core orbitals. Figure 5 illustrates the sensitivity of the computed

Complex	B^{66}LYP	SRC	Exp.
$[MnO_4]^{1-}$	6548	-	-
	6544	6537	6538
	6526	6520	6522
$[MnN(CN)_4]^{2-}$	6540	6535	6535
	6538	6532	6533
	6524	6522	6525
$Cr(CO)_6$	5986	5981	5984
	5982	5976	5980
$[Cr(NH_3)_6]^{3+}$	5993	5987	5988
	5986	5982	-
	5974	5970	5973

TABLE IV. Computed B^{66}LYP and SRC emission energies for the complexes studied. Experimental data from references[10,11].

band profiles to the quality of the basis set. There is a clear improvement in the computed spectra when basis sets larger than 6-31G* and u6-31G* are used. However, the band profiles computed with the Ahlrichs VTZ basis set are very similar to those of the considerably larger cc-pCVTZ basis set. The Ahlrichs VTZ basis set is a moderately sized basis set that can be applied to study much larger systems.

IV. CONCLUSION

TDDFT with the TDA has been applied to the calculation of X-ray emission spectra of transition metal complexes by using a reference determinant with a core hole in the metal 1s orbital, and applied to study the XES of the $[MnO_4]^{1-}$, $[MnN(CN)_4]^{2-}$, $Cr(CO)_6$ and
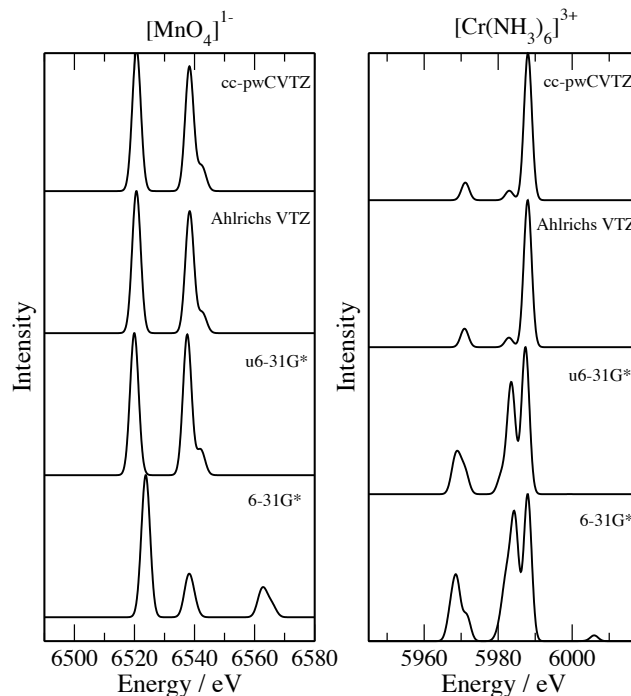
FIG. 5. Variation of the band profiles computed with the SRC exchange-correlation functional with basis set. Spectra have been shifted to align with the cc-pCVTZ spectra.

$[Cr(NH_3)_6]^{3+}$ complexes. This a relatively straightforward computational method to use and in conjunction with the FO approximation, where there is no relaxation of the orbitals of the intermediate state, it gives spectra that are similar to existing approaches to simulate XES of systems of this type. The computed transition energies show a large dependence on the quality of the basis set used, and to achieve close agreement with experimental spectra it is necessary to use high quality basis with additional basis functions to describe the core orbitals. To compute X-ray emission spectra with the correct energy scale allowing a direct comparison of experiment and theory without the need to shift the computed spectra to match experiment requires the relaxation of the core ionised state to be included and the use of specifically designed functionals with increased amounts of HF exchange. The FO approximation has a smaller effect on the computed spectral band profiles than changes in the exchange-correlation functional, and variations in the spectra between different functional are present whether the FO approximation is applied or not. Two types of exchange-correlation functional parameterised for the XES of molecules involving elements from the first and second rows of the periodic table were studied. The first is a modified

19

hybrid functional with 66% HF exchange and the second a range-separated functional with an increased component of HF exchange in the short range only. While the computed transition energies are a lot closer to experiment, the hybrid functional gives band profiles that show a poorer agreement with experiment than standard functionals. The SRC functional represents a compromise giving transition energies close to experiment and spectral band profiles that are nearly as accurate as those from standard functionals such as B3LYP. The bands observed in the valence to core region have been correlated with the degree of metal p character in the molecular orbitals comprising the constituent transitions, and it is shown that some of the deviation from experiment in the computed band profiles can be associated with incorrect mixing of transitions introduced by the TDDFT eigenvector. Further improvements in the calculations such as a more accurate treatment of relativistic effects, going beyond the dipole approximation in the calculation of the intensities and inclusion of transition metal complex XES data in the functional parameterisation should improve the agreement with experiment further.

V. ACKNOWLEDGMENTS

REFERENCES

[1] J. van Bokhoven, *Phys. Chem. Chem. Phys.* **12**, 5502-5502 (2010).

[2] B.D. Patterson and R. Abela, *Phys. Chem. Chem. Phys.* **12**, 5647-5652 (2010).

[3] G. Smolentsev, A.V. Soldatov, J. Messinger, K. Merz, T. Weyhermüller, U. Bergmann, Y. Pushkar, J. Yano, V.K. Yachandra and P. Glatzel, *J. Am. Chem. Soc.* **131**, 13161-13167 (2009).

[4] N. Lee, T. Petrenko, U. Bergmann, F. Neese and S. DeBeer, *J. Am. Chem. Soc.* **132**, 9715-9727 (2010).

[5] J.C. Swarbrick, Y. Kvashnin, K. Schulte, K. Seenivasan, C. Lamberti and P. Glatzel, P. *Inorg. Chem.* **49**, 8323-8332 (2010).

[6] M.A. Beckwith, M. Roemelt, M.-N. Collomb, C. DuBoc, T.-C. Weng, U. Bergmann, P. Glatzel, F. Neese, and S. DeBeer, *Inorg. Chem.* **50**, 8397-8409 (2011).

[7] C.J. Pollock and S. DeBeer, *J. Am. Chem. Soc.* **133**, 5594-5601 (2011).

[8] A.J. Atkins, M. Bauer and C. R. Jacob, *Phys. Chem. Chem. Phys.* **15**, 8095-8105 (2013).

[9] M.U. Delgado-Jaime, S. DeBeer and M. Bauer, *Chem. Eur. J.* **19**, 15888-15897 (2013).

[10] E.R. Hall, C.J. Pollock, J. Bendix, T.J. Collins, P. Glatzel and S. DeBeer, *J. Am. Chem. Soc.* **136**, 10076-10084 (2014).

[11] S.N. MacMillan, R.C. Walroth, D.M. Perry, T.J. Morsing and K.M. Lancaster, *Inorg. Chem.* **54**, 205-214 (2015).

[12] K.M. Lancaster, M. Roemelt, P. Ettenhuber, Y. Hu, M.W. Ribbe, F. Neese, U. Bergmann and S. DeBeer, *Science* **334**, 974-977 (2011).

[13] F. de Groot, *Coord. Chem. Rev.* **249**, 31-63 (2005).

[14] H. Ågren and J. Nordgren, *Theoret. Chim. Acta* **58**, 111-119 (1981).

[15] H. Ågren, R. Arneberg, J. Müller, and R. Manne, *Chem. Phys.* **83**, 53-67 (1984).

[16] Ågren, H.; Flores-Riveros, A.; Jørgen, H.; Aa Jensen, H.J. *Physica Scripta* **1989**, *40*, 745-750.

[17] A. Flores-Riveros and H. Ågren, *Physica Scripta* **44**, 442-445 (1991).

[18] J.P. Coe and M.J. Paterson, *Theor. Chem. Acc.* **134**, 58 (2015).

[19] L. Triguero, L. G.M. Pettersson and H. Ågren, *J. Phys. Chem. A* **102**, 10599-10607 (1998).

[20] A. Föhlisch, J. Hasselström, P. Bennich, N. Wassdahl, O. Karis, A. Nilsson, L. Triguero, M. Nyberg and L.G.M. Pettersson, *Phys. Rev. B* **61**, 16229-16240 (2000).

[21] J. Gladh, H. Öberg, J. Li, M.P. Ljungberg, A. Matsuda, H. Ogasawara, A. Nilsson, L.G.M. Pettersson and H. Öström *J. Chem. Phys.* **136**, 034702 (2012).

[22] M. Leetmaa, M.P. Ljungberg, A. Lyubartsev, A. Nilsson and L.G.M. Pettersson, *J. Electron Spectrosc. Relat. Phenom.* **177**, 135-157 (2010).

[23] T. Tokushima, Y. Harada, Y. Horikawa, O. Takahashi, Y. Senba, H. Ohashif, L.G.M. Pettersson, A. Nilsson, A. and S. Shin, *J. Electron Spectrosc. Relat. Phenom.* **177**, 192-205 (2010).

[24] T.E. Meehan, J. McColl and F.P. Larkins, *J. Electron Spectrosc. Relat. Phenom.* **73**, 283-292 (1995).

[25] T.R. Walsh, T.E. Meehan and F.P. Larkins, *J. Phys. B.: At. Mol. Opt. Phys.* **29**, 207-220 (1996).

[26] M.P. Ljungberg, J.J. Mortensen and L.G.M. Pettersson, *J. Electron Spectrosc. Relat. Phenom.* **184**, 427-439 (2011).

[27] M.P. Ljungberg, L.G.M. Pettersson and A. Nilsson, *J. Chem. Phys.* **134**, 044513 (2011).

[28] N.A. Besley and F. Asmuruf, *Phys. Chem. Chem. Phys.* **12**, 12024-12039 (2010).

[29] N.A. Besley, *Chem. Phys. Lett.* **542**, 42-46 (2012).

[30] J.D. Wadey and N.A. Besley, *J. Chem. Theory Comput.* **10**, 4557-4564 (2014).

[31] O.V. Ershova and N.A. Besley, *Chem. Phys. Lett.* **513**, 179-183 (2011).

[32] S. Hirata and M. Head-Gordon, *Chem. Phys. Lett.* **314**, 291-299 (1999).

[33] Y. Zhang, S. Mukamel, M. Khalil and N. Govind, *J. Chem. Theory Comput.* **11**, 5804-5809 (2015).

[34] T.Noro, M. Sekiya and T. Koga, *Theor. Chem. Acc.* **131**, 1124 (2012).

[35] A. Nakata, Y. Imamura, T. Ostuka and H. Nakai, *J. Chem. Phys.* **124**, 094105 (2006).

[36] A. Nakata, Y. Imamura and H. Nakai, *J. Chem. Theory Comput.* **3**, 1295-1305 (2007).

[37] N.A. Besley and A. Noble, *J. Phys. Chem. C* **111**, 3333-3400 (2007).

[38] N.A. Besley, M.J.G. Peach and D.J. Tozer, *Phys. Chem. Chem. Phys.* **11**, 10350-10358 (2009).

[39] A.T.B. Gilbert, N.A. Besley and P.M.W. Gill, *J. Phys. Chem. A* **112**, 13164-13171 (2008).

[40] N.A. Besley, A.T.B. Gilbert and P.M.W. Gill, *J. Chem. Phys.* **130**, 124308 (2009).

[41] F.A. Asmuruf and N.A. Besley, *Chem. Phys. Lett.* **463**, 267-271 (2008).

[42] A.D. Becke, *J. Chem. Phys.* **98**, 5648-5652 (1993).

[43] P.J. Stephens, F.J. Devlin, C.F. Chabalowski and M.J. Frisch, *J. Phys. Chem.* **98**, 11623-11627 (1994).

[44] A.D. Becke, *Phys. Rev. A* **38**, 3098-3100 (1988).

[45] J.P. Perdew, *Phys. Rev. B* **37**, 785 (1986).

[46] C.T. Lee, W.T. Yang and R.G. Parr, *Phys. Rev. B* **37**, 785-789 (1988).

[47] P.A.M. Dirac, *Proc. Cam. Phil. Soc.* **26**, 376-385 (1930).

[48] S.H. Vosko, L. Wilk and M. Nusair, *Can. J. Phys.* **58**, 1200-1211 (1980).

[49] R. Krishan, J.S. Binkley, R. Seeger and J.A. Pople, *J. Chem. Phys.* **72**, 650-654 (1980).

[50] T.H. Dunning Jr., *J. Chem. Phys.* **90**, 1007-1023 (1989).

[51] A. Schafer, H. Horn and R. Ahlrichs, *J. Chem. Phys.* **97**, 2571-2577 (1992).

[52] D.E. Woon and T.H. Dunning Jr., *J. Chem. Phys.* **98**, 1358-1371 (1993).

[53] N.B. Balabanov and K.A. Peterson, K.A. *J. Chem. Phys.* **123**, 064107 (2005).

[54]Y. Shao, Z. Gan, E. Epifanovsky, A.T.B. Gilbert, M. Wormit, J. Kussmann, A.W. Lange, A. Behn, J. Deng, X. Feng, et al. *Mol. Phys.* **113**, 184-215 (2005).

[55]F. deGroot, *Coord. Chem. Rev.* **249**, 31-63 (2005).

[56]D. Robinson and N.A. Besley, *Phys. Chem. Chem. Phys.* **12**, 9667-9676 (2010).

[57]N.A. Besley and D. Robinson, *Faraday Discussions* **148**, 55-70 (2011).

[58]M. Schindler and W. Kutzelnigg, *J. Chem. Phys.* **76**, 1919-1933 (1982).

[59]S. Bernadotte, A.J. Atkins and C.R. Jacob, *J. Chem. Phys.* **137**, 204106 (2012).

[60]G. Capano, T.J. Penfold, N.A. Besley, C.J. Milne, M. Reinhard, H. Rittmann-Frank, P. Glatzel, R. Abela, U. Rothlisberger, M. Chergui and I. Tavernelli, *Chem. Phys. Lett.* **580**, 179-184 (2013).